VARIATIONAL SCHEME FOR ANALYSIS OF TORSION OF EMBEDDED NONUNIFORM ELASTIC BARS

By A. P. S. Selvadurai,[1] M. ASCE, and R. K. N. D. Rajapakse[2]

ABSTRACT: This paper develops a novel solution scheme for the analysis of the transfer of an axially symmetric torque from a nonuniform elastic bar into a layered elastic halfspace. The torsional deformation of the bar is specified by a set of kinematically admissible functions that are indeterminate to within a set of arbitrary constants. The embedded bar-elastic halfspace system is represented by extended halfspace and a fictitious bar. The fictitious traction distribution on the extended halfspace due to a specified displacement field is determined by a discretization procedure. The results of the analysis is used to develop the total potential energy functional for the bar-elastic halfspace loading system. The minimization of the functional determines explicitly the torsional deformation field. The numerical results presented in the paper illustrate the manner in which the torsional stiffness of the bar is influenced by its nonuniformity and its relative rigidity.

INTRODUCTION

The study of torsional response of flexible bars and inclusions embedded in elastic media is of interest to several branches of engineering. Flexible piers are used quite extensively as structural foundations for isolated structures, e.g., power transmission towers, housings of solar cell arrays, offshore beacon structures, and as anchors for floating structures [Fig. 1(*a*)]. These pier-type structures can be subjected to significant torsion which is induced by off-axis loadings. In its conventional form, these structural foundations are usually cylindrical in shape. On occasions they can be constructed with a tapered or nonuniform section [Fig. 1(*b* and *c*)]. The analytical study of torsion of cylindrical bars embedded in elastic media has received some attention. For example, Keer and Freeman (4) examined the problem of the torsional loading of an infinitely long elastic bar with a finite protruding length, embedded in a homogeneous isotropic elastic halfspace. Poulos (10) investigated the torsion of uniform piles embedded in an elastic halfspace by employing a discretization scheme. An exact analytical formulation of the problem of the torsion of a rigid cylindrical pier embedded in a layered elastic halfspace was presented by Luco (6). In the study by Luco (6), integral representations were used to reduce the problem to the approximate numerical solution of two integral equations. In the work by Randolph (12), an approximate solution based on a simplified assumption of the stress field is used to examine the torsional loading of the embedded pier. Selvadurai (13) investigated the

[1]Prof. and Chmn., Dept. of Civ. Engrg., Carleton Univ., Ottawa, Ont., Canada K15 5B6.

[2]Asst. Prof., Dept. of Civ. Engrg., Univ. of Manitoba, Winnipeg, Manitoba, A3T 2N2, Canada.

Note. Discussion open until March 1, 1988. To extend the closing date one month, a written request must be filed with the ASCE Manager of Journals. The manuscript for this paper was submitted for review and possible publication on May 21, 1985. This paper is part of the ***Journal of Engineering Mechanics***, Vol. 113, No. 10, October, 1987. ©ASCE, ISSN 0733-9399/87/0010-1534/$01.00. Paper No. 21883.

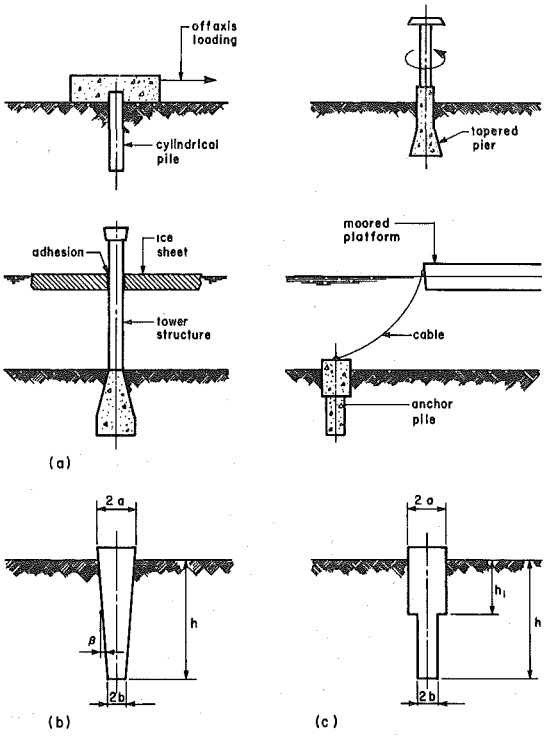

FIG. 1. Torsional loading of Pier-Type Structures. (*a*) Pier-Type Structures; (*b*) Tapered Bar; (*c*) Step-Tapered Bar

torsion of a hemispheroidal rigid inclusion embedded in a homogeneous isotropic elastic halfspace. Karasudhi, et al. (3) presented a solution to the problem of torsion of a finite elastic bar that is partially embedded in a layered elastic halfspace. The method employed was similar to that presented by Muki and Sternberg (8) for the axial load transfer problem; the resulting Fredholm integral equation was solved by employing a numerical scheme. Recently, Rajapakse and Selvadurai (11) used a discretization technique to solve the class of problems pertaining to the torsional loading of nonuniform and hollow rigid piers embedded in a layered elastic halfspace.

An examination of the literature indicates that the problem of the torsion of nonuniform elastic cylinders embedded in an elastic medium merits further consideration. The methodology adopted in the paper focuses on the application of a variational procedure to investigate the torsional load transfer problem. Variational methods serve as powerful mathematical tools for the development of solutions to many complicated boundary value problems in engineering mechanics where exact analytical solutions or refined numerical schemes cannot be readily developed. Although the mathematical basis of the variational schemes in elastostatics is well established, they have not been applied, extensively, to the study of load

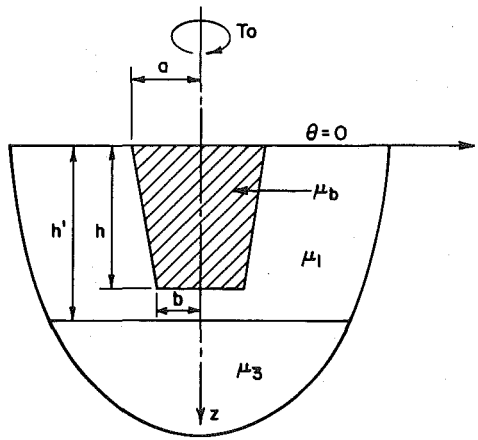

FIG. 2. Idealized Bar-Elastic Halfspace System

transfer problems. In the context of elastostatic contact problems, variational schemes have been applied quite effectively to the study of unilateral and bilateral contact problems, see, e.g., Duvaut and Lions (1), Villagio (17), Panagiotopoulos (9), Kikuchi and Oden (5), Selvadurai (13,14). For example, Selvadurai (14) examined the classical problem of axisymmetric contact between an elastic plate and a transversely isotropic elastic halfspace by employing a variational scheme. The variational scheme yielded results that compared very favorably with existing solutions, based on numerical schemes. Selvadurai (13) also examined the flexural interaction between an embedded disc inclusion and an isotropic elastic infinite space by employing a variational procedure.

The primary purpose of the present paper is to illustrate the application of a variational scheme to the study of either the torsional stiffness of a non-uniform bar or the torsional load transfer between a nonuniform bar and an elastic halfspace region (Fig. 2). The method is essentially numerical in character but utilizes the advantages of a variational formulation. It is assumed that due to the application of the torsional load, the bar experiences a deformation which includes: (1) A rigid body rotation of the entire inclusion; and (2) rotations that vary along the length of the bar. The latter deformation is specified to within a set of unknown constant coefficients. The bar itself is assumed to experience only Saint-Venant-type torsional stresses. The surrounding elastic medium, which is in adhesive contact with the bar, deforms according to the imposed deformation field. In the analysis, the bar-elastic halfspace system is represented by an extended elastic medium (i.e., a medium without a cylindrical cavity) and a fictitious elastic bar with an appropriate elastic modulus as considered in Ref. 3. A discretized form of the fictitious tractions induced at the fictitious contact surface in the extended medium due to the imposed deformation can be computed by using a fundamental solution related to the axisymmetric torsional loading of the interior of a halfspace by a ring load. Using these techniques, it is possible to develop a total potential energy functional for the bar-elastic medium system. This functional includes the elastic energy of the extended halfspace, the elastic energy of the fictitious bar, and the potential energy of the applied torsional loads.

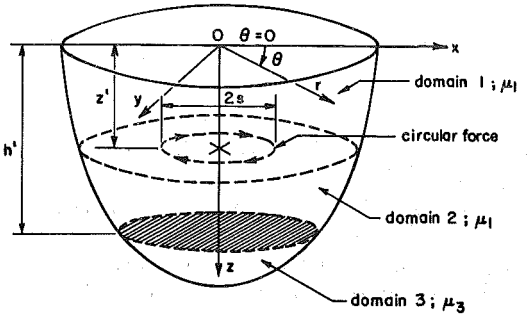

FIG. 3. Interior Loading of Elastic Halfspace by Concentrated Circular Force

This functional is indeterminate to within the arbitrary constants characterizing the deformation of the bar. A minimization of the total potential energy functional can be used to determine these arbitrary constants. This numerical procedure is used to examine the torsional response of uniform and nonuniform elastic bars embedded in a layered elastic halfspace.

Fundamental Solution

Fig. 3 shows the layered elastic halfspace system. The cylindrical polar coordinate system (r, θ, z) is chosen such that the z-axis is normal to the free surface of the halfspace region. The class of problems under consideration possesses a state of symmetry about the z-axis, and the functions involved are independent of azimuthal coordinate θ. Owing to the state of symmetry imposed by axisymmetric torsion, the displacements u and w in the r and z-directions, respectively, vanish. Also, in the absence of body forces, the nonzero displacement component v in θ-direction is governed by the displacement equation of equilibrium:

$$\frac{\partial^2 v}{\partial r^2} - \frac{v}{r^2} + \frac{1}{r}\frac{\partial v}{\partial r} + \frac{\partial^2 v}{\partial z^2} = 0 \quad \text{..... (1)}$$

The nonzero stress components $\sigma_{r\theta}$ and $\sigma_{\theta z}$ referred to the cylindrical polar coordinate system can be expressed in the form:

$$\sigma_{\theta z} = \mu \frac{\partial v}{\partial z} \quad \text{..... (2a)}$$

$$\sigma_{r\theta} = \mu \left(\frac{\partial v}{\partial r} - \frac{v}{r}\right) \quad \text{..... (2b)}$$

where μ = the linear elastic shear modulus of the medium.

The general solution of Eq. 1 is obtained by employing a Hankel transform development (with respect to the radial coordinate) of the governing differential equation (Eq. 1). Following Sneddon (16), it can be shown that the generalized solution for the displacement v can be expressed in the form:

$$v(r, z) = \int_0^\infty (Ae^{-\xi z} + Be^{\xi z})J_1(\xi r)\, d\xi \quad \text{(3)}$$

where J_1 = the first order Bessel function of the first kind; and $A(\xi)$ and $B(\xi)$ = arbitrary functions that should be determined by invoking appropriate boundary and continuity conditions. At this stage, it is convenient to non-dimensionalize the problem by defining a, which denotes the radius of the embedded bar at the plane $z = 0$, as a unit length.

In the ensuing section, which deals with variational formulation, we need to obtain the distribution of tractions along the bar-elastic medium interface due to a deformation imposed along the bar-elastic medium interface. To the writers' knowledge, there is no exact analytical solution for the problem related to the determination of the traction distribution generated due to an imposed state of deformation at the contact surface for a nonuniform inclusion embedded in a halfspace.

In view of this difficulty, it is necessary to seek an alternative to evaluation of true contact stresses at the interface. An efficient way to achieve this objective is to follow Refs. 3 and 8 and decompose the original problem shown in Fig. 2 into an extended halfspace and a fictious bar with a modified modulus as shown in Fig. 4. Fictitious tractions of equal magnitude but opposite directions are applied on surfaces S^* and S^{**} such that displacements in direction along surfaces S^* and S^{**} are equal. The advantage of this decomposition is that it allows the determination of magnitude of fictitious contact tractions due to a specified displacement field on S^{**} through the use of only displacement influence functions for a halfspace without a cylindrical void. For the purposes of a variational formulation, the most efficient and accurate way to compute the fictitious traction distribution $T^*(z)$ is to discretize the fictitious contact surface S^{**} in the extended halfspace and to seek a numerical solution. The surface S^{**} is discretized into ring elements of equal width as shown in Fig. 4. The total number of elements employed to discretize the surface S^{**} is denoted by N_t. It is found that any surface S^{**} could be discretized by the three different types of elements, namely, the vertical (VE), inclined (IE), and base (BE) elements shown in Fig. 5. The traction within each element is distributed as shown in Fig. 5.

In order to obtain a numerical solution for the traction at discrete points along the surface S^{**}, it is necessary to compute the displacement in the θ-direction at a point P_i (r_i, z_i) on the surface S^{**} due to the action of unit tractions over domains corresponding to different elements shown in Fig. 5. To obtain this solution, we require the fundamental solution corresponding to a concentrated circular force in the θ-direction applied at the interior of a layered halfspace (Fig. 3). Referring to Fig. 3, by defining a fictitious plane at $z = z'$, we can reduce the problem to one that has three domains. The superscript i (i = 1, 2, 3) is used to identify the quantities associated with each domain. The displacement field in each domain has the general form given by Eq. 1 consisting of functions $A_i(\xi)$ and $B_i(\xi)$. In the domain 3, however, to ensure regularity of displacements and stresses derived from Eq. 1, the term $B_3(\xi) = 0$. The remaining five functions $A_i(\xi)$ (i = 1, 2, 3); $B_i(\xi)$ (i = 1, 2) are determined from the following boundary and continuity conditions:

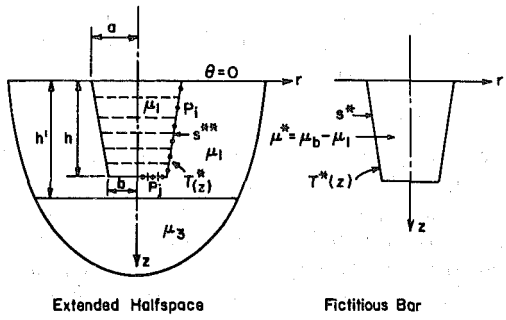

FIG. 4. Decomposition of Bar-Elastic Halfspace System

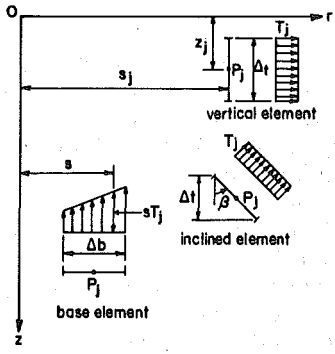

FIG. 5. Basic Elements Used to Model Surface S^{**}

$$\sigma_{\theta z}^{(1)}(r, 0) = 0 \quad \text{(4a)}$$

$$v^{(1)}(r, z') = v^{(2)}(r, z') \quad \text{(4b)}$$

$$\sigma_{\theta z}^{(1)}(r, z') - \sigma_{\theta z}^{(2)}(r, z') = \delta(r - s) = \int_0^\infty s\xi J_1(\xi s) J_1(\xi r)\, d\xi \quad \text{(4c)}$$

$$v^{(2)}(r, h') = v^{(3)}(r, h') \quad \text{(4d)}$$

$$\sigma_{\theta z}^{(2)}(r, h') = \sigma_{\theta z}^{(3)}(r, h') \quad \text{(4e)}$$

These conditions are valid for the case $z' < h'$. The corresponding expressions for the case $z' > h'$ could be obtained easily. The solution of the resulting system of simultaneous equations leads to the expressions for the unknown functions A_i and B_i. Explicit expressions for the displacements corresponding to each domain are given by Rajapakse and Selvadurai (11). Upon derivation of the fundamental solution it is necessary to derive the displacement distributions f_{ij} at point P_i (r_i, z_i) due to tractions of unit magnitude distributed over vertical, base, and inclined elements (j), as shown in Fig. 5. The expressions for f_{ij} could be derived by integrating the fundamental solution along the width of each element. It is noted that the fundamental solution could be integrated analytically for tractions

applied over the vertical and base elements. For the inclined element, however, a numerical integration has to be employed across the element width to compute f_{ij}. The expressions for f_{ij} are given in Appendix I.

Variational Formulation

Consider a layered elastic halfspace with an embedded tapered elastic bar as shown in Fig. 2. The bar can terminate either within the elastic layer or within the elastic halfspace region. It is assumed that the layer and the halfspace are perfectly bonded at the plane $z = 0$ and that the bar is perfectly bonded to the surrounding medium. Finally, it is assumed that due to the application of a torque T_0, the elastic bar experiences a state of deformation which is expressed in the form

$$v(r, z) = r \sum_{n=1}^{N} \omega_n e^{-(n-1)z/h} \quad \text{..... (5)}$$

where $\omega_1, \ldots, \omega_N$ = arbitrary constants. It may be noted that the displacement field (Eq. 5) exhibits Saint-Venant-type decay as z increases.

In view of the decomposition of the original problem as shown in Fig. 4, the displacement field of the fictitious bar is considered as identical to the real bar as given by Eq. 5. However the deformation of the region V in the extended halfspace is not totally compatible with that of fictitious bar. As in many classical load-transfer problems, limited displacement compatibility must be enforced. In the present study, compatibility is assumed only between surfaces S^* and S^{**}. This is also a consequence of the fact that three-dimensional modeling is adopted for the extended medium, whereas the fictitious bar is treated using a relevant one-dimensional theory. However, the effect due to this limited compatibility could be considered negligible for bars with high length-radius ratios.

Considering Eq. 5, the torsional energy of the fictitious bar (U_T) as shown in Fig. 4 can be expressed as

$$U_T = \sum_{n=1}^{N} \sum_{m=1}^{N} D_{mn} \omega_n \omega_m \quad \text{..... (6)}$$

where

$$D_{mn} = \frac{\pi \mu_b^*}{4h^2} (n-1)(m-1) \sum_{p=1}^{5} \left[\frac{(p-1)!}{c_{mn}^p} - e^{-hc_{mn}} \sum_{q=0}^{p} \frac{(p-1)!}{q!} \frac{h^q}{c_{mn}^{p-q}} \right] \lambda p \quad (7)$$

$$\text{and} \quad c_{mn} = \frac{(m+n-2)}{h} \quad \text{..... (8a)}$$

$$\lambda_1 = a^4 \quad \text{..... (8b)}$$

$$\lambda_2 = 4a^3 \tan \beta \quad \text{..... (8c)}$$

$$\lambda_3 = 6a^2 \tan^2 \beta \quad \text{..... (8d)}$$

$$\lambda_4 = 4a \tan^3 \beta \quad \text{..... (8e)}$$

$$\lambda_5 = \tan^4 \beta \quad \text{..... (8f)}$$

$$\mu_b^* = \mu_b - \mu_1 \quad \text{..... (8g)}$$

For a step-tapered bar, as shown in Fig. 1(*c*), the torsional energy U_T of the fictitious bar can also be expressed in the form of Eq. 6, except that the relevant expression for D_{mn} takes the form

$$D_{mn} = \frac{\pi \mu_b^*}{4h} \frac{(n-1)(m-1)}{(n+m-2)} [a^4(1 - e^{-(m+n-2)h_1/h})$$

$$+ b^4(1 - e^{-(m+n-2)h_1/h}) - b^4 e^{-(m+n-2)}] \quad \text{..... (9)}$$

The strain energy of the extended elastic medium due to the deformation imposed along the surface S^{**} could be computed if the tractions acting on the fictitious contact surface are known. These tractions are computed by imposing independently the deformation corresponding to each term of Eq. 5 with $\omega_1, \omega_2, \ldots \omega_N$ equal to unity and then formulating the flexibility equation for the fictitious contact surface. Let us denote the traction generated on the jth element due to the nth term of Eq. 5 with $\omega_n = 1$ as T_{nj}. Using the influence function f_{ij} defined previously, we can write the following flexibility equation to determine T_{nj}:

$$[f_{ij}]\{T_{nj}\} = \{V_{ni}\}; (i,j = 1, \ldots, N_t), (n = 1, \ldots, N) \quad \text{..... (10)}$$

$$\text{where} \quad \{T_{nj}\} = \langle T_{n1}, \ldots, T_{ni}, \ldots, T_{N_t} \rangle^T \quad \text{..... (11a)}$$

$$\{V_{ni}\} = \langle \beta_{n1} r_1, \ldots, \beta_{ni} r_i, \ldots, \beta_{N_t} r_{N_t} \rangle^T \quad \text{..... (11b)}$$

$$\text{and} \quad \beta_{ni} = e^{-(n-1)z_i/h} \quad \text{..... (11c)}$$

The solution of systems of simultaneous equations results in $\{T_{nj}\}$ for $n = 1, \ldots, N$. The tractions acting on the jth element at the fictitious contact surface S^{**} is denoted by T_j^*; this can be expressed in the form

$$T_j^* = \sum_{n=1}^{N} \omega_n \gamma_j T_{nj} \quad \text{..... (12)}$$

where $\gamma_j = 1$ if the jth element is a vertical or inclined element; and $\gamma_j = r_j$ is the jth element is a base element. (Note that no summation is implied on the repeated indices in Eq. 12). The strain energy of the extended halfspace region can be expressed as

$$U_{HS} = \frac{1}{2} \int \int_{S^{**}} T^*(r, z) v(r, z)\, ds \quad \text{..... (13)}$$

where S^{**} = the fictitious contact surface in the extended elastic medium; and $T^*(r, \theta, z)$ = the continuous form of the traction acting on the surface S^{**}, which we have obtained in the discrete form as given by Eq. 12. In view of Eqs. 5 and 12, Eq. 13 can be written as

$$U_{HS} = \pi \sum_{n=1}^{N} \sum_{m=1}^{N} \sum_{j=1}^{N_t} \omega_n \omega_m T_{nj} \gamma_j e^{*-(m-1)z_j/h} \Delta t_j \quad \text{..... (14)}$$

where $\gamma_j^* = r_j^2$, if jth element is VE or IE; $\gamma_j^* = r_j^3$, if jth element is BE; $\Delta t_j = \Delta z/\cos\beta$ if jth element is VE or IE; and $\Delta t_j = \Delta r$, if jth element is BE.

The total potential energy functional of the system U, can be written as

$$\tilde{U} = U_T + U_{HS} - T_0 \sum_{n=1}^{N} \omega_n \quad \text{..... (15)}$$

By minimizing the total potential energy functional, i.e., $\partial \tilde{U}/\partial \omega_i = 0$, ($i = 1, 2, \ldots, N$), the following system of linear simultaneous equations is obtained:

$$\sum_{n=1}^{N} \omega_n \left\{ 2D_{ni} + \pi \sum_{j=1}^{N_t} [\gamma_j^* T_{nj} e^{-(i-1)z_j/h} + \gamma_j^* T_{ij} e^{-(n-1)z_j/h}] \Delta t_j \right\} = T_0;$$

$(i = 1, \ldots, N)$ ..... (16)

Note that $D_{ni} = 0$ if $(n + i) = 2$.

A solution of the system of simultaneous equations given by Eq. 16 gives the numerical values of arbitrary constants $\omega_1, \ldots, \omega_N$. The displacements of the bar and fictitious traction acting at the surface S^{**} due to the applied torque T_0 could be computed by using Eqs. 5 and 12.

As an alternative to the function basis given by Eq. 5, we can consider a polynomial variation of displacement v along the length of the bar as follows:

$$v(r, z) = r \sum_{n=1}^{N} \omega_n \left(\frac{z}{h}\right)^{n-1} \quad \text{..... (17)}$$

Following procedures similar to those outlined earlier, it can be shown that the minimization of the total potential energy functional $\tilde{U}$ results in the following system of simultaneous equations:

$$\sum_{n=1}^{N} \omega_n \left\{ 2D_{ni} + \pi \sum_{j=1}^{N_t} \gamma_j^* \left[T_{nj} \left(\frac{z_j}{h}\right)^{i-1} + T_{ij} \left(\frac{z_j}{h}\right)^{n-1} \right] \Delta t_j \right\}$$

$$= T_0 \delta_{1i}; \qquad (i = 1, \ldots, N) \quad \text{..... (18)}$$

where, for a tapered bar [Fig. 1(*b*)]

$$D_{ni} = \frac{\pi \mu_b^*}{4} \frac{(n-1)(i-1)}{h^{(n+i-2)}} \left[\frac{a^4 h^{n+i-3}}{(n+i-3)} + \frac{4a^3 h^{n+i-2}}{(n+i-2)} \tan \beta \right.$$

$$\left. + \frac{6a^2 h^{n+i-1}}{(n+i-1)} \tan^2 \beta + \frac{4ah^{n+i}}{(n+i)} \tan^3 \beta + \frac{h^{n+i+1}}{(n+i+1)} \tan^4 \beta \right] \quad \text{..... (19)}$$

for a step tapered bar [Fig. 1(*c*)]

$$D_{ni} = \frac{\pi \mu_b^*}{4h} \frac{(n-1)(i-1)}{(n+i-3)} \left[(a^4 - b^4) \left(\frac{h_1}{h}\right)^{n+i-3} + b^4 \right] \quad \text{..... (20a)}$$

$$D_{ni} = 0; \qquad \text{if} \quad n + i - 3 = 0 \quad \text{..... (20b)}$$

where δ_{ij} = Kronecker's delta function. Note that simultaneous equation systems given by Eqs. 16 and 18 are symmetrical. For the case of an infinitely rigid bar $\omega_2, \ldots, \omega_N = 0$, Eqs. 16 and 18 reduce to

$$\omega_1\left(2\pi \sum_{j=1}^{N_t} \gamma_j T_{1j} \Delta t_j\right) = T_0 \quad \text{..... (21)}$$

Numerical Solution Scheme

The numerical solution of Eq. 10 involves the computation of influence function f_{ij} given in Appendix I. It may be noted that the influence function f_{ij} consists of several integrals of the Lipschitz-Hankel type, defined by

$$I(p, q; \lambda) = \int_0^\infty J_p(\xi r) J_q(\xi s) e^{-n\xi} \xi^\lambda \, d\xi \quad \text{..... (22)}$$

It may be noted that all Lipschtz-Hankel-type integrals associated with f_{ij} could be expressed in terms of elliptic integrals. These elliptic integrals may be evaluated with high precision using currently available scientific and mathematical software. It is observed that a major proportion of the computational effort is spent on the evaluation of f_{ij} and the solution of simultaneous equation systems given by Eq. 10. In contrast, the computational effort involved in the solution of the simultaneous equations generated by the variational procedure is relatively small. Based on the solution procedure described in the preceding sections, the writers have developed a computer code to evaluate the stiffness of elastic bars. The input parameters include the shear modulus of the bar, the shear modulus of the top layer and the halfspace regions, the geometry of the bar, and the value of N_t and N. The program computes the displacements and tractions at discrete points located on the contact surface.

Results and Conclusions

In the parametric study, we consider the case where the length of the bar and that of the layer are equal. Since we have considered exponential as well as polynomial forms for the unknown displacement function, it is necessary to compare the performance of both function bases in terms of convergence of results. Table 1 presents the results obtained, for both exponential and polynomial forms, for an elastic bar ($h/a = 5$; and $\mu_b/\mu_1 = 10$) embedded in a homogeneous halfspace. Both schemes give results that are in close agreement with the corresponding results given by Karasudhi et al. (3). However, by assuming an exponential variation, convergence is achieved with only a few terms of the assumed displacement function. For this reason, all the results presented in the ensuing sections are based on the exponential form given by Eq. 5.

TABLE 1. Comparison of Convergence of $3T_0/16\mu_3 a^3\phi_0$ Obtained from Different Displacement Functions: $h/a = 5.0$; $\mu_b/\mu_1 = 10$; $\alpha = 1.0$; $b/a = 1.0$; $N_t = 45$

Form of assumed displacement function (1)	$3T_0/16\mu_3 a^3\phi_0$					
	$N = 2$ (2)	$N = 3$ (3)	$N = 4$ (4)	$N = 5$ (5)	$N = 6$ (6)	$N = 7$ (7)
Exponential	3.79	2.94	2.83	2.82	2.82	2.82
Polynomial	4.32	3.10	2.94	2.86	2.82	2.82

TABLE 2. Convergence of $3T_0/16\mu_3 a^3\phi_0$ for Elastic Pile ($\mu_b/\mu_3 = 10$) Embedded in Homogeneous Elastic Soil; $h/a = 5$

N (1)	$3T_0/16\mu_3 a^3\phi_0$		
	$N_s = 10$; $N_b = 2$ (2)	$N_s = 20$; $N_b = 5$ (3)	$N_s = 40$; $N_b = 5$ (4)
2	3.61	3.70	3.71
4	2.82	2.82	2.82
6	2.81	2.81	2.82

Another important factor to be considered is the effect of the number of elements considered in discretizing the surface S^{**} on the convergence of results. Table 2 presents the values of $3T_0/16\mu_3 a^3\phi_0$ for three different combination values of N_s and N_b and also for varying N. Note that N_s and N_b denote the number of elements used to model the shaft and base of the S^{**}, respectively. Again convergence is established with $N \simeq 6$.

Randolph (12) presented an approximate equation to compute the torsional stiffness of an elastic pile. In this analysis, it was assumed that the variation of v is such that the term $\partial\sigma_{\theta z}/\partial z$ appearing in the equilibrium equation is negligible and that the base of the pile behaves as a rigid circular disc bonded to a halfspace region. The latter assumption essentially follows the theoretical developments of the Reissner-Sagoci problem. Following procedures similar to those employed by Randolph (12) it is possible to derive an approximate torque-twist relationship for a uniform cylindrical elastic bar embedded in a layered elastic halfspace. It is found that

$$\frac{3T_0}{16\mu_3 a^3\phi_0} = \frac{\left[1 + \left(\frac{3\pi}{4\alpha}\right)\left(\frac{h}{a}\right)\frac{\tanh(\beta)}{\beta}\right]}{\left[1 + \left(\frac{32\alpha}{3\pi\lambda}\right)\left(\frac{h}{a}\right)\frac{\tanh(\beta)}{\beta}\right]} \quad \ldots\ldots\ldots\ldots\ldots\ldots\ldots\ldots\ldots\ldots \quad (23)$$

TABLE 3. $3T_0/\mu_3 a^3\phi_0$ for Elastic Piles Obtained from Variational Scheme and Approximate Results Given by Eq. 23

μ_b/μ_1 (1)	$\alpha = 1.0$				$\alpha = 2.0$			
	$h/a = 5.0$		$h/a = 30.0$		$h/a = 5.0$		$h/a = 30.0$	
	Variational solutions (2)	Eq. 23 (3)	Variational solutions (4)	Eq. 23 (5)	Variational solutions (6)	Eq. 23 (7)	Variational solutions (8)	Eq. 23 (9)
5	2.00	1.86	2.17	1.86	1.15	0.93	1.11	0.93
10	2.83	2.63	2.90	2.63	1.42	1.32	1.39	1.32
100	7.80	7.59	8.42	8.33	4.12	3.87	4.32	4.16
1,000	12.36	11.86	26.24	26.11	6.57	6.32	13.41	13.06
10,000	13.28	12.68	59.78	58.02	7.03	6.82	29.84	29.26
100,000	13.29	12.77	70.97	69.96	7.05	6.88	36.03	35.45

where $\beta = \frac{h}{a}\left(\frac{8}{\lambda}\right)^{1/2}$ ..... (24)

$\alpha = \frac{\mu_3}{\mu_1}$ ..... (25)

and $\lambda = \frac{\mu_b}{\mu_1}$ ..... (26)

For a homogeneous halfspace, Eq. 23 reduces to the form given by Randolph (12) for an infinitely rigid bar: $\tanh(\beta)/\beta \rightarrow 1$ and $\lambda \rightarrow \infty$. Consequently, Eq. 23 reduces to the simplified formula given by Luco (6) for a uniform rigid cylinder embedded in a layered halfspace. Table 3 presents a comparison of the numerical results for $3T_0/16\mu_3 a^3\phi_0$ obtained from the variational scheme presented in this study and the approximate results given by Eq. 23. Except for very flexible bars, the results agree reasonably closely with each other. By nature of the assumptions em-

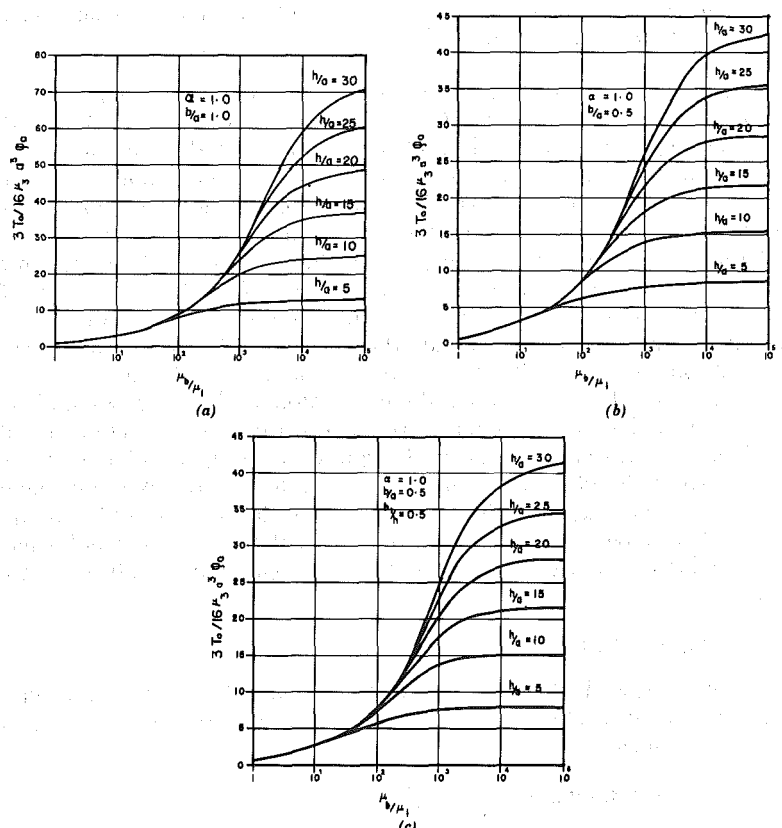

FIG. 6. Influence of Bar Flexibility and Bar Aspect Ratio on Torsional Stiffness: Homogeneous Elastic Solid

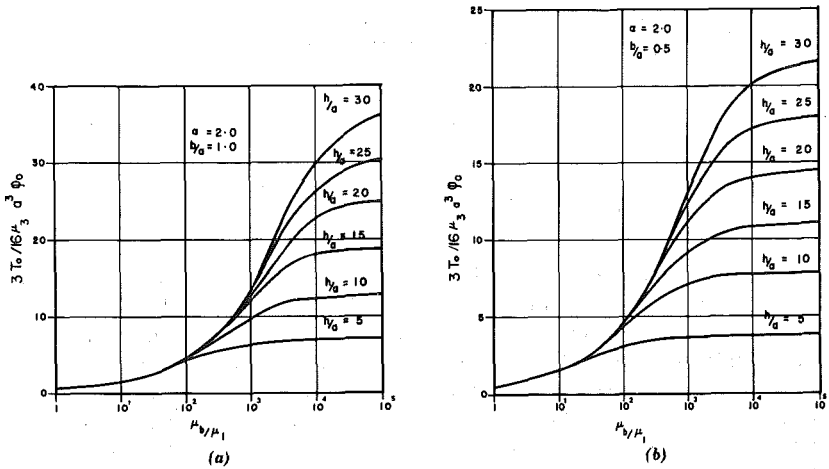

FIG. 7. Influence of Bar Flexibility and Bar Aspect Ratio on Torsional Stiffness: Nonhomogeneous Elastic Solid

ployed in its derivation, Eq. 23 should always give a lower-bound value for the torque-twist relationship. Fig. 6 shows the variation of $3T_0/16\mu_3 a^3\phi_0$ with the length-to-radius ratio and the flexibility of the bar for uniform, tapered, and step-tapered elastic bars, respectively, embedded in a homogeneous elastic halfspace. The corresponding results for uniform and tapered bars embedded in layered halfspace are given in Fig. 7. It is noted that for very flexible bars ($\mu_b/\mu_1 \leq 20$) the torsional stiffness is almost independent of length if $h/a \geq 5$. However, as μ_b/μ_1 increases, curves for the stiffness follow different paths according to the length-to-radius ratio of the bar. It is also observed that the presence of uniform tapering or step-tapering has a significant influence on the torsional stiffness.

Finally, it can be concluded that the variational scheme presented in this study is an efficient and accurate procedure for solving torsion transfer problems. It is also found that, in the light of convergence characteristics, an exponential function as given by Eq. 5 is computationally more efficient than the polynomial basis. The method illustrated in this study could be extended to solve a variety of problems involving rigid and deformable irregular inclusion regions embedded in isotropic and anisotropic elastic media.

Acknowledgments

The work described in this paper was supported in part by a research grant (A3866) awarded by the Natural Sciences and Engineering Research Council of Canada.

Appendix I. Influence Function f_{ij}

The influence function f_{ij} obtained from integrating the fundamental solution is found to be

For a vertical element, $(z_j + \Delta t/2) \leq h'$:

$$f_{ij} = \frac{1}{2\mu_1(1+\alpha)} \sum_{m=1}^{5} a_m [-(1+\alpha)\phi_m(1, 1; -1) + (1-\alpha)\psi_m(1, 1; -1)]_{z'=z_j^1}^{z'=z_j^2}; (z_i \le z_j^1) \quad \text{..... (27)}$$

$$f_{ij} = \frac{1}{2\mu_1(1+\alpha)} \sum_{m=1}^{5} \times a_m [-(1+\alpha)\bar{\phi}_m(1, 1; -1) + (1-\alpha)\bar{\psi}_m(1, 1; -1)]_{z'=z_j^1}^{z'=z_j^2}; (z_i \ge z_j^2) \quad (28)$$

$$f_{ij} = \frac{1}{2\mu_1(1+\alpha)} \sum_{m=1}^{5} \times a_m \{[-(1+\alpha)\bar{\phi}_m(1, 1; -1) + (1-\alpha)\bar{\psi}_m(1, 1; -1)]_{z'=z_j^1}^{z'=z_i} + [-(1+\alpha)\phi_m(1, 1; -1) + (1-\alpha)\psi_m(1, 1; -1)]_{z'=z_i^2}^{z'=z_j^2}\};$$

$$(z_j^1 < z_i < z_j^2) \quad \text{..... (29)}$$

$$f_{ij} = \frac{1}{\mu_1(1+\alpha)} \sum_{m=1}^{5} a_m [\phi_m(1, 1; -1)]_{z'=z_j^1}^{z'=z_j^2}; \quad (z_i \ge h') \quad \text{..... (30)}$$

For a vertical element, $(z_j - \Delta t/2) \ge h'$:

$$f_{ij} = \frac{1}{\mu_1(1+\alpha)} \sum_{m=1}^{5} a_m [\phi_m(1, 1; -1)]_{z'=z_j^1}^{z'=z_j^2}; \quad (z_i \le h') \quad \text{..... (31)}$$

$$f_{ij} = \frac{1}{2\alpha\mu_1(1+\alpha)} \sum_{m=1}^{5} \times a_m [-(1+\alpha)\phi_m(1, 1; -1) + (1-\alpha)\psi_m(1, 1; -1)]_{z'=z_j^1}^{z'=z_j^2};$$

$$(h' \le z_i \le z_j^1) \quad \text{..... (32)}$$

$$f_{ij} = \frac{1}{2\alpha\mu_1(1+\alpha)} \sum_{m=1}^{5} \times a_m [-(1+\alpha)\bar{\phi}_m(1, 1; -1) + (1-\alpha)\bar{\psi}_m(1, 1; -1)]_{z'=z_j^1}^{z'=z_j^2};$$

$$(h' \le z_j^2 \le z_i) \quad \text{..... (33)}$$

$$f_{ij} = \frac{1}{2\alpha\mu_1(1+\alpha)} \sum_{m=1}^{5} \times a_m \{[-(1+\alpha)\bar{\phi}_m(1, 1; -1) + (1-\alpha)\bar{\psi}_m(1, 1; -1)]_{z'=z_j^1}^{z'=z_i} + [-(1+\alpha)\phi_m(1, 1; -1) + (1-\alpha)\psi_m(1, 1; -1)]_{z'=z_i^2}^{z'=z_j^2}\};$$

$$(z_j^1 < z_i < z_j^2) \quad \text{..... (34)}$$

For a base element, $z_j \le h'$:

J. Eng. Mech., 1987, 113(10): 1534-1550

$$f_{ij} = \frac{1}{2\mu_1(1+\alpha)} \sum_{m=1}^{5} a_m \left[(1+\alpha)\phi_m(1, 2; -1)\right.$$

$$\left. + (1-\alpha)\psi_m(1, 2; -1)\right]_{s=sj1}^{s=sj2}; \qquad (z_i \le h') \quad \ldots\ldots (35)$$

$$f_{ij} = \frac{1}{\mu_1(1+\alpha)} \sum_{m=1}^{5} a_m \left[\phi_m(1, 2; -1)\right]_{s=sj1}^{s=sj2}; \qquad (z_i \ge h') \quad \ldots\ldots (36)$$

For a base element, $z_j \ge h'$:

$$f_{ij} = \frac{1}{\mu_1(1+\alpha)} \sum_{m=1}^{5} a_m \left[\phi_m(1, 2; -1)\right]_{s=sj1}^{s=sj2}; \quad (z_i \le h') \quad \ldots\ldots (37)$$

$$f_{ij} = \frac{1}{2\alpha\mu_1(1+\alpha)} \sum_{m=1}^{5} a_m \left[(1+\alpha)\phi_m(1, 2; -1)\right.$$

$$\left. + (1-\alpha)\psi_m(1, 2; -1)\right]_{s=sj1}^{s=sj2}; \qquad (z_i \ge h') \quad \ldots\ldots (38)$$

For an inclined element, $(z_j + \Delta t/2) \le h'$:

$$f_{ij} = \frac{1}{2\mu_1(1+\alpha)} \sum_{m=1}^{5} a_m \left\{ \int_{zj'}^{zj^2} \left[(1+\alpha)\phi_m(1, 1; 0)\right.\right.$$

$$\left.\left. + (1-\alpha)\psi_m(1, 1; 0)\right] \frac{dz'}{\cos\beta} \right\}; \qquad (z_i \le h') \quad \ldots\ldots (39)$$

$$f_{ij} = \frac{1}{\mu_1(1+\alpha)} \sum_{m=1}^{5} a_m \left[\int_{zj'}^{zj^2} \phi_m(1, 1; 0) \frac{dz'}{\cos\beta} \right]; \quad (z_i \ge h') \quad \ldots\ldots (40)$$

For an inclined element, $(z_j - \Delta t/2) \ge h'$:

$$f_{ij} = \frac{1}{\mu_1(1+\alpha)} \sum_{m=1}^{5} a_m \left[\int_{zj'}^{zj^2} \phi_m(1, 1; 0) \frac{dz'}{\cos\beta} \right]; \quad (z_i \le h') \quad \ldots\ldots (41)$$

$$f_{ij} = \frac{1}{2\alpha\mu_1(1+\alpha)} \sum_{m=1}^{5} a_m \left\{ \int_{zj'}^{zj^2} \left[(1+\alpha)\phi_m(1, 1; 0)\right.\right.$$

$$\left.\left. - (1-\alpha)\psi_m(1, 1; 0)\right] \frac{dz'}{\cos\beta} \right\}; \qquad (z_i \ge h') \quad \ldots\ldots (42)$$

where $\phi_m(p, q; \lambda) = s^q[I_{1m}(p, q; \lambda) + I_{2m}(p, q; \lambda)]$ ..... (43)

$\bar{\phi}_m(p, q; \lambda) = s^q[I_{1m}(p, q; \lambda) - I_{2m}(p, q; \lambda)]$ ..... (44)

$\psi_m(p, q; \lambda) = s^q[I_{3m}(p, q; \lambda) + I_{4m}(p, q; \lambda)]$ ..... (45)

$\bar{\psi}_m(p, q; \lambda) = s^q[I_{3m}(p, q; \lambda) - I_{4m}(p, q; \lambda)]$ ..... (46)

and $I_{1m}(p, q; \lambda) = \int_0^\infty J_p(\xi r_i) J_q(\xi s) \xi^\lambda e^{-\xi[z_i + z' + 2(m-1)h']}\, d\xi$ ..... (47)

$$I_{2m}(p, q; \lambda) = \int_0^\infty J_p(\xi r_i) J_q(\xi s) \xi^\lambda e^{-\xi[|z_i - z'| + 2(m-1)h']} \, d\xi \quad \text{..... (48)}$$

$$I_{3m}(p, q; \lambda) = \int_0^\infty J_p(\xi r_i) J_q(\xi s) \xi^\lambda e^{-\xi[|2h' - z_i - z'| + 2(m-1)h']} \, d\xi \quad \text{..... (49)}$$

$$I_{4m}(p, q; \lambda) = \int_0^\infty J_p(\xi r_i) J_q(\xi s) \xi^\lambda e^{-\xi[2h' - |z_i - z'| + 2(m-1)h']} \, d\xi \quad \text{..... (50)}$$

$$[f(t)]_{t=t_2}^{t=t_1} = f(t_1) - f(t_2) \quad \text{..... (51)}$$

$$z_j^1 = z_j - \frac{\Delta t}{2} \quad \text{..... (52)}$$

$$z_j^2 = z_j + \frac{\Delta t}{2} \quad \text{..... (53)}$$

$$s_j^1 = s_j - \frac{\Delta b}{2} \quad \text{..... (54)}$$

$$s_j^2 = s_j + \frac{\Delta b}{2} \quad \text{..... (55)}$$

The constants a_m appearing in the Eqs. 27–55 correspond to the expansion of denominator appearing in the fundamental solution for a circular concentrated torque at the interior of a layered halfspace, i.e.

$$\frac{(1+\alpha)}{[(1+\alpha) - (1-\alpha)e^{-2\xi h}]} = \sum_{m=1}^{M} a_m e^{-2(m-1)h} \quad \text{..... (56)}$$

where $\alpha = \mu_3/\mu_1$.

The values of a_m could be determined by applying the integral least square method.

Appendix II. References

1. Duvaut, G., and Lions, J. L. (1976). *Inequalities in mechanics and physics*, Springer-Verlag, Berlin, West Germany.
2. Kalker, J. J. (1977). "Variational principles of contact elastostatics," *J. Inst. Math. and Its Applications*, 20, 199–219.
3. Karasudhi, P., Rajapakse, R. K. N. D., and Hwang, B. Y. (1984). "Torsion of a long cylindrical elastic bar partially embedded in a layered elastic half space," *Int. J. Solids and Struct.*, 20(1), 1–11.
4. Keer, L. M, and Freeman, N. J. (1970). "Load transfer problem for an embedded shaft in torsion," *J. Appl. Mech.*, ASME, 37, 504–512.
5. Kikuchi, N., and Oden, J. T. (1979). "Contact problems in elasticity," *TICOM Report 79-8*, Univ. of Texas, Austin, Tx.
6. Luco, J. E. (1976). "Torsion of a rigid cylinder embedded in an elastic half space," *J. Appl. Mech.*, ASME, 43, 419–423.
7. Muki, R. (1960). "Asymmetric problems of the theory of elasticity for a semi-infinite solid and a thick plate," *Progress in solid mechanics*, I. N. Sneddon and R. Hill, eds., Vol. 1, North Holland Pub. Co., Amsterdam, Netherlands, 285–290.

8. Muki, R., and Sternberg, E. (1970). "Elastostatic load transfer to a half space from a partially embedded axially loaded rod," *Int. J. Solids and Struct.*, 6(1), 69–90.
9. Panagiotoupoulos, P. D. (1977). "On the unilateral contact problem of structures with non-quadratic strain energy density," *Int. J. Solids and Struct.*, 13, 253–261.
10. Poulos, H. G. (1975). "Torsional response of piles," *J. Geotech. Engrg. Div.*, ASCE, 101(GT10), 1019–1035.
11. Rajapakse, R. K. N. D., and Selvadurai, A. P. S. (1985). "Torsional stiffness of non-uniform and hollow rigid piers embedded in isotropic elastic media," *Int. J. Numer. and Analyt. Methods in Geomech.*, 9(6), 525–539.
12. Randolph, M. F. (1981). "Piles subjected to torsion," *J. Geotech. Engrg. Div.*, ASCE, 107(GT8), 1095–1111.
13. Selvadurai, A. P. S. (1979). "An energy estimate of the flexural behaviour of a circular foundation embedded in an isotropic elastic medium," *Int. J. Numer. and Analyt. Methods in Geomech.*, 3, 285–292.
14. Selvadurai, A. P. S. (1980). "Elastic contact between a flexible circular plate and a transversely isotropic elastic halfspace," *Int. J. Solids and Struct.*, 16, 167–176.
15. Selvadurai, A. P. S. (1984). "Torsional stiffness of rigid piers embedded in isotropic elastic soils," *Laterally loaded deep foundations: analysis and performance*, J. A. Langer, E. Mosley, and C. Thompson, eds. ASTM, 49–55.
16. Sneddon, I. N. (1951). *Fourier transforms*, McGraw-Hill, New York, N.Y.
17. Villaggio, P. (1977). *Qualitative methods in elasticity*, Noordhoff International Publishing, Leyden, Netherlands.